

## Synthesis and Studies on Photophysical Properties of Rhodamine Derivatives for Bioimaging Applications

Balasaheb D. Vanjare,<sup>†</sup> Prasad G. Mahajan,<sup>†</sup> Nilam C. Dige,<sup>‡</sup> Abdul Rehman Phull,<sup>‡,§</sup>  
Song Ja Kim,<sup>‡</sup> and Ki Hwan Lee<sup>†,\*</sup>

<sup>†</sup>Department of Chemistry, Kongju National University, Gongju 32588, Republic of Korea.

\*E-mail: khlee@kongju.ac.kr

<sup>‡</sup>Department of Biological Sciences, Kongju National University, Gongju 32588, Republic of Korea

<sup>§</sup>Department of Biochemistry, Shah Abdul Latif University, Khairpur 66020, Pakistan

Received January 30, 2019, Accepted April 5, 2019

Rhodamine derivatives have been persistently used as fluorescent/solvatochromic dyes in various areas. For example, they are used as a labeling agent in biotechnology and a chemosensor. Also, rhodamine derivatives are used for cell imaging experiment. Herein, we report on the synthesis of fluorescent derivatives based on rhodamine B (**RHB1**, **RHB2**, and **RHB3**). We confirmed the structures and purities of the synthesized probes *i.e.*, **RHB1**, **RHB2**, and **RHB3** by using analytical technique's *viz.* <sup>1</sup>H NMR, <sup>13</sup>C NMR, Mass and FT-IR followed by exploring spectroscopic properties by using fluorescence/UV absorption spectroscopy. The effect of solvents on the fluorescence and absorption properties of the synthesized compounds has been comprehensively studied using a series of solvent. In addition, synthesized **RHB1**, **RHB2**, and **RHB3** were found to be non-toxic against the cancer cell (MDA-MB-231). It is clear from the result of the conventional fluorescence microscopy that probe **RHB2** exhibits significant optical properties as compared with those of **RHB1** and **RHB3**.

**Keywords:** Rhodamine derivatives, Photophysical properties, Cell imaging, Cytotoxicity.

### Introduction

During the past decade, fluorescent probes are used for the selective detection of chemical species in the environmental contaminants and labels of targeting molecules. For the qualifying conditions in the selection of organic dyes as a fluorescent probe, it must display the finest fluorescence response when it irradiated in the visible range and less lethal to the living cells and tissues.<sup>1–3</sup> The common structural feature in several fluorophores is a conjugated  $\pi$ -system and having both electrons donating and withdrawing group.<sup>4–6</sup> Rhodamine and its derivatives form a family of multipurpose functional dyes, which have been extensively used due to their excellent photophysical properties.<sup>7–10</sup> Additionally, Rhodamine derivatives go through two forms *i.e.* spirocyclic and open rings form. The spirocyclic forms (non-fluorescent, colorless) exhibit limited  $\pi$  bond conjugated arrangement, whereas the open ring form (fluorescent, pink) shows exhaustive signals in the absorption and fluorescence spectroscopy due to extended large  $\pi$ -conjugated systems.<sup>11–14</sup> Rhodamine derivatives are massively used in the field of the bioimaging and biosensors because of their outstanding optical properties such as, quantum yield, molar absorption coefficient and photostability. For instance, Rhodamine 123 has been selectively designated for restraining the active mitochondria and used

as a marker for mitochondrial membrane potential (MMP).<sup>15</sup>

In the last decade, numerous research groups were engaged in development of the conjugated organic systems possessing rhodamine core.<sup>16–18</sup> Besides, for the construction of the extra conjugation by  $\pi$  system, the design of the inflexible rings in the rhodamine derivatives can have more probabilities of shifting the absorption/emission spectra to a longer wavelength. However, most of the rhodamine derivatives have absorption and emission wavelengths below 600 nm. Additionally, owing to the lack of molecular rotation in the xanthenes ring, it raises the rigidity of the molecule, which increases the fluorescence quantum yield.<sup>19</sup>

In the present work, we have synthesized three different derivatives of Rhodamine (**RHB1**, **RHB2**, and **RHB3**) and its optical properties have been studied in different solvents. The comparison syntax of the synthesized three dyes for the photophysical properties in various solvent systems indicates **RHB2** with higher-extinction coefficient, quantum yield and Stokes shift than those of other dyes *i.e.*, **RHB1** and **RHB3**. Moreover, these compounds were employed for cell imaging experiment, which reveals that **RHB2** shows superior fluorescence imaging against cancer cells (MDA-MB-231) because of their structural variation, significant optical properties, higher Stokes shift value, and low cytotoxicity as compared to those of **RHB1** and **RHB3**.

### Experimental Section

**Materials.** Rhodamine B, hydrazine hydrate, 2-amino-5-{4-bromophenyl}-1,3,4-thiadiazole, 4–5 diazafluoren-9-one, 4- amino benzaldehyde, 2-(*1H*-benzotriazol-1-yl)-1,1,3,3,–tetramethyluronium hexafluorophosphate (HBTU), N, N-diisopropylethylamine (DIPEA) and N,N-dimethyl formamide (DMF) were obtained from Sigma Aldrich (Munich, Germany). Ethanol, methanol (MeOH), ethyl acetate (EtOAc), dichloromethane (DCM), acetonitrile (ACN), dimethyl sulfide (DMSO), and acetone used in these experiments were purchased from Samchun Chemicals (Daejeon, South Korea) until and unless mentioned.

**Equipment.** Fluorescence spectra and UV–Visible spectra of all the samples were recorded at room temperature by using FS-2 fluorescence spectrophotometer (Scinco, Seoul, Korea) and Shimadzu spectrophotometer (Kyoto, Japan), respectively. FT-IR measurements were accomplished on Frontier IR (Perkin Elmer, Santa Clara, CA, USA) spectrometer using KBr pellets. <sup>1</sup>H NMR (400 MHz) and <sup>13</sup>C NMR (125 MHz) were recorded on the Bruker Avance 400 and 100 MHz spectrophotometer (Billerica, MA, USA) and TMS is used as an internal standard. The LC–MS mass spectra were recorded on 2795/ZQ2000 (Waters, Milford, MA, USA) spectrometer. All the melting points of the synthesized compounds were measured on Fisher Scientific (Pittsburgh, PA, USA) melting point apparatus.

**Quantum Yield Measurements.** In absorption and fluorescence experiment, a stock solution of **RHB1**, **RHB2**, and **RHB3** were prepared using different spectroscopic grade pure solvents at room temperature. 1 cm path length of the cells used for the absorption and emission study. All the fluorescence experiments were completed by keeping slit width constant *i.e.*, 5 × 5 nm. Each fluorescence and absorption spectra were taken after 60 min. The fluorescence quantum yield was calculated by using Eq. (1), given below.<sup>20,21,26</sup>

$$\Phi_{sample} = \Phi_{ref} \times \frac{OD_{ref} \times A_{sample} \times \eta_{sample}^2}{OD_{sample} \times A_{ref} \times \eta_{ref}^2} \quad (1)$$

where *A* signifies the integrated area of the fluorescence spectrum and *OD* signifies the optical density of the probe at the excitation wavelength,  $\eta$  is the refractive index of the solvent used for the experiment. Quinine sulphate in 0.1 M sulfuric acid was used as the reference standard ( $\Phi_f$ ) = 0.546.<sup>22</sup>

**Culturing of Cancer Cells (MDA-MB-231) and Cell Imaging Studies.** The cancer cells were maintained and grown in DMEM medium supplemented with FBS (10%), antibiotics (streptomycin, 50 µg/mL and penicillin, 50 units/mL). Furthermore, previously cultured and maintained cells were seeded in 35 mm culture plate at the density of 1 × 10<sup>5</sup> per plate. Following day, the medium was replaced with fresh medium and cells were left to grow

until the confluence of the cells reached approximately 65%. Subsequently, cells were treated with and without 10 µM of **RHB1**, **RHB2**, and **RHB3** for 2 h in the presence of growth medium. The treated and untreated sample cells were washed with cold PBS buffer two to three times. Finally, fluorescence images of green light excited cells were taken by using a fluorescence microscope (BX51, Olympus, and Tokyo, Japan). In order to compare the fluorescence intensities during imaging investigations, all settings such as exposure time, contrast and brightness were maintained at the same level. The experiment was repeated three times and performed 37 °C in a CO<sub>2</sub> incubator.

**Cytotoxicity Assessment by MTT Assay.** The cytotoxic effect of samples was investigated through MTT assay on the viability of cancer (MDA-MB-231) cells. MDA-MB-231 cells were plated at a density of 2.5 × 10<sup>4</sup> cells/well on 96-well plate. The cells were grown for 12 h and the growth medium was changed. The cells grew until the confluence of the cells reached up to 75%. Subsequently, grown cells were exposed with and without **RHB1**, **RHB2**, and **RHB3** at the concentration of 10 µM for 2 and 12 h in the existence of a growth medium. After the treatment of specific experimental times *i.e.*, 2 and 12 h, 10 µL of MTT reagent 1 (MTT, 10 mg/mL) was added in each well and subjected to incubate for 4 h. Subsequently, each well was added with 100 µL of MTT reagent 2 or solubilization buffer (DMSO and 10% SDS with 0.01 N HCl) and subjected to incubate in similar conditions for 12 h. Finally, absorbance was measured at 595 nm by using assay plate reader (Molecular Devices, Sunnyvale, CA, USA).<sup>23,24</sup> The experiment was repeated three times and the non-treated cell was considered 100% viable and used as the control.

### Synthesis and Spectral Characterization Techniques

**Synthesis of 2-(5-(4-Bromophenyl)-1, 3, 4-thiadiazol-2-yl)-3', 6'-bis (diethyl amino) spiro [isindoline-1, 9'-xanthen]-3-one (RHB1).** Rhodamine B (0.5 g, 1.043 mmol), 2-amino-5-{4-bromophenyl}-1, 3, 4-thiadiazole (0.30 g, 1.148 mmol), and HBTU (0.48 g, 1.25 mmol) was taken in DMF (5 mL) and stirred the reaction mixture for 10 min at ambient temperature. Di-isopropylethylamine (0.6 mL, 3.13 mmol) was added and continued the reaction for 4 h. Synthesis route of **RHB1** is as shown in Scheme 1. The reaction mixture was quenched with ice-cold water and extracted with ethyl acetate. The ethyl acetate layer was washed with water/brine, distilled out the organic layer and purified by using column chromatography DCM: methanol (9:1) as an eluent to afford a light pink solid, Yield: 76%, M. P: 225–229 °C; Figure S1 (Supporting Information): <sup>1</sup>H NMR (DMSO-*d*<sub>6</sub>, 400 MHz)  $\delta$  (ppm): 8.07 (d, *J* = 7.5 Hz, 1H), 7.87–7.78 (m, 2H), 7.77–7.61 (m, 2H), 7.77–7.61 (m, 4H), 7.19 (d, *J* = 7.6 Hz, 1H), 6.41 (d, *J* = 2.5 Hz, 2H), 6.36 (d, *J* = 8.9 Hz, 2H), 6.23 (dd, *J* = 8.9, 2.6 Hz, 2H) 3.29 (t, 8H), 1.07 (q, 12H); Figure S2: <sup>13</sup>C NMR (DMSO-*d*<sub>6</sub>,

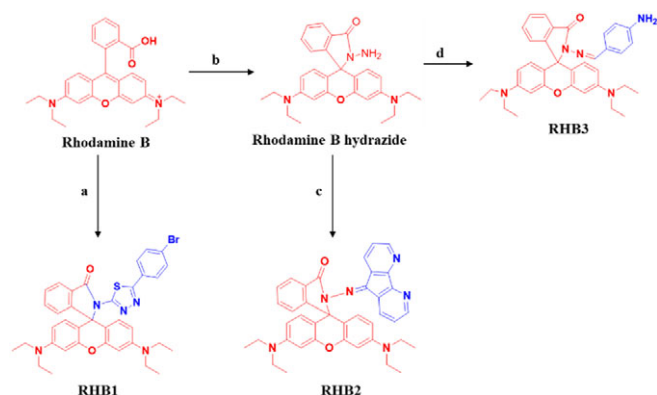
125 MHz)  $\delta$  (ppm): 165, 162, 154, 156, 148, 145, 149, 136, 133, 125, 124, 108, 106, 97, 68, 44, 12; Figure S3: IR (KBr)  $\nu$ /cm: 2966.98, 2927.43, 2293.87, 1709.67, 1634.95, 1613.95, 913.55, 903.98, 817.52; Figure S4: LC-MS: 682.4  $m/z$  ( $M + 2$ ).

### Synthesis of 2-(9H-4-5 Diazafluorene)-3', 6'-bis (diethyl amino) spiro [isoindoline-1, 9'-xanthen]-3-one (RHB2).

As demonstrated in Scheme 1, **RHB2** compound was synthesized by reaction of rhodamine hydrazide **B** with 4-5 diazafluoren-9-one. Previously reported synthetic route has been employed for the preparation of rhodamine B hydrazide.<sup>25</sup> Rhodamine B hydrazide (0.5 g, 1.09 mmol) and 4-5 diazafluoren-9-one (0.19 g, 1.09 mmol) were dissolved in DMF (4 mL), stirred for 12 h at ambient temperature (monitored by TLC). The ice-cold water was added and stirred for 10–15 min. The received solid was filtered and washed with ice-cold water. Obtained solid was dried and subsequently purified by silica gel chromatography using DCM:methanol (0–3%) as the eluent to afford **RHB2** as an off-white solid, yield: 85%, M.P: 148–150 °C; Figure S5: <sup>1</sup>H NMR (DMSO-*d*<sub>6</sub>, 400 MHz)  $\delta$  (ppm): 8.9–8.51 (2H, m), 8.30–8.07 (2H, m), 7.76 (1H, s), 7.6–7.5 (5H, m), 7.10–6.9 (2H, m), 6.56–6.1 (4H, m), 3.5–3.23 (8H, q), 1.08 (12H, t). Figure S6: <sup>13</sup>C NMR (DMSO-*d*<sub>6</sub>, 125 MHz)  $\delta$  (ppm): 164, 162, 157, 155, 150, 133, 132, 130, 128, 1126, 122, 110, 108, 99, 64, 44, 12; Figure S7: IR (KBr)  $\nu$ /cm: 2940.85, 2292.49, 1694.51, 1460.94, 1429.32, 903.90, 809.07. Figure S8: LC-MS: 621.5  $m/z$  ( $M + 1$ ).

### Synthesis of 2-(4-Aminobenzylideneamino)-3', 6'-bis (diethyl amino) spiro [isoindoline-1, 9'-xanthen]-3-one (RHB3).

Initially, 0.5 g (1.09 mmol) of Rhodamine B hydrazide and 0.13 g (1.09 mmol) of 4-amino benzaldehyde was dissolved in 6 mL ethanol by stirring for 12 h at ambient temperature (monitored by TLC). The solid was obtained by filtering and subjected to wash with cold ethanol. The crude solid was purified by using column chromatography using (DCM:methanol) as the eluent to afford a



**Scheme 1.** Reagents and conditions: (a) 2-amino-5-[4-bromophenyl]-1, 3, 4-thiadiazole, HBTU, DIEPA, DMF, RT/4 h. (b) Hydrazine hydrate, ethanol, reflux (c) 4-5 diazafluoren-9-one, ethanol, ambient temperature, 12 h. (d) 4-Amino benzaldehyde, ethanol, ambient temperature, 12 h.

yellow solid, yield: 72%, M.P: 213–215 °C; Figure S9: <sup>1</sup>H NMR (DMSO-*d*<sub>6</sub>, 400 MHz)  $\delta$  (ppm): 1.07 (t, 12H, -NCH<sub>2</sub>CH<sub>3</sub>), 3.30 (q, 8H, -NCH<sub>2</sub>CH<sub>3</sub>), 4.26 (s, 2H, Ar-NH<sub>2</sub>), 6.0–7.0 (m, 6H, xanthenene-H), 6.3–6.5 (m, 4H, ArH), 7.78 (dd, 1H, ArH), 7.5 (s, 1H, -CH=N), 7.4–7.5 (m, 3H, ArH). Figure S10: <sup>13</sup>C NMR (DMSO-*d*<sub>6</sub>, 125 MHz)  $\delta$  (ppm): 166, 155, 152, 149, 133, 131, 128, 129, 126, 124, 108, 106, 98, 65, 44, 13. Figure S11: IR (KBr)  $\nu$ /cm: 3022.11, 2969.56, 2891.16, 2343.56, 2300.80, 1692.09, 1633.94, 1613.84, 1548.27, 1396.01, 967.13. Figure S12: LC-MS: 560.5  $m/z$  ( $M + 1$ ).

## Results and Discussions

### UV Visible Absorption and Fluorescence Spectroscopy.

The influence on UV-Vis absorption and fluorescence emission spectra of  $1 \times 10^{-4}$  mol/L solution of compounds **RHB1**, **RHB2**, and **RHB3** in a variety of solvents at room temperature by considering an extensive range of polarity including non-polar, polar, polar protic, and polar aprotic solvents are presented in Figures 1–2, and 3, showing the resultant statistics given in Table 1. The absorption of both **RHB1** (Figure 1(a)) and **RHB3** (Figure 3(a)) were found to be very less penetrating for the variation in the polarity of the solvents as compared to that of **RHB2**. For all-different polarity of solvents, two prominent absorption band was observed in the UV region.<sup>26,35</sup> The absorption maximum of **RHB1** changes from 560 nm (DCM) to 562 nm (methanol), except in polar aprotic solvents (acetone) other solvents do not show an absorption band. The absorption maximum of **RHB2** ranges from 560 nm

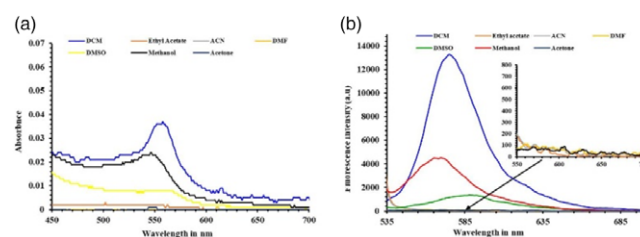


**Figure 1.** The absorption (a) and fluorescence (b) spectra of the **RHB1** at the concentration of  $1 \times 10^{-4}$  mol/L in different solvents.

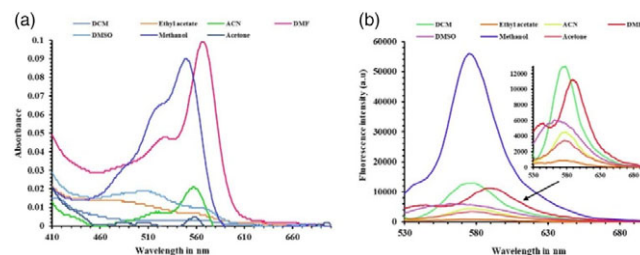


**Figure 2.** The absorption (a) and fluorescence (b) spectra of the **RHB2** at the concentration of  $1 \times 10^{-4}$  mol/L in different solvents.

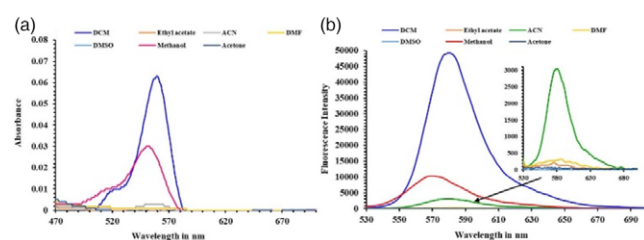


**Figure 3.** The absorption (a) and fluorescence (b) spectra of the **RHB3** at the concentration of  $1 \times 10^{-4}$  mol/L in different solvents.

(DCM) to 568 nm (DMF), polar protic solvents have no consequence on the absorption of **RHB2**. The absorption maximum of **RHB3** compound in DMF and DCM solvents is around 560 nm, but it is slightly blue shifted in polar protic solvents *i.e.*, 554 nm in methanol. The excellent fluorescence properties are the main feature of the present synthesized compounds. Figures 1(b), 2(b), and 3(b) illustrate the emission spectra of the **RHB1**, **RHB2**, and **RHB3**, respectively. The fluorescence emission bands are broad in nature and shows wide spectral visible region from 500 to 650 nm for **RHB1**, from 520 to 650 nm for **RHB2**, and from 540 to 650 nm for **RHB3** in a variety of solvent. This band assigned to the  $S_1 \rightarrow S_0$  electronic transition. In all three compounds, the effect of the solvent polarity on the emission spectra was more prominent than absorption spectrum, it is due to the intramolecular charge transfer (ICT) effect.<sup>28,35</sup> The change in the polarity of solvent used for fluorescence emission study induces the

change in the little spectral shift by 2–20 nm for all the compounds.<sup>27–30</sup>

Table 1 shows the photophysical parameters including absorption and fluorescence maxima, molar extinction coefficients, Stokes shifts and fluorescence quantum yields for each rhodamine derivatives. The absorption spectra display broad band in the range from 540 to 620 nm for all these three compounds. Moreover, a high molar absorption coefficient ranges from 80 to  $360 \text{ M}^{-1} \text{ cm}^{-1}$ , 40 to  $1000 \text{ M}^{-1} \text{ cm}^{-1}$  and 30 to  $630 \text{ M}^{-1} \text{ cm}^{-1}$  was observed for the compounds **RHB1**, **RHB2**, and **RHB3**, respectively. The review of the data in Table 1 displays that the location of the  $\pi\text{-}\pi^*$  absorption band considerably depends on the polarity of the solvents.<sup>3</sup>

Moreover, the fluorescence band is affected by changing the solvent polarity.<sup>31–34</sup> While relating these three derivatives and its fluorescence emission response against series of solvent reveals that, **RHB2** derivative shows maximum fluorescence emission intensity as compared with **RHB1** and **RHB3**, except in DCM solvent as shown in Figure 2. Furthermore, the compound **RHB1** shows very less fluorescence emission intensity in EtOAc, ACN, DMF, and acetone as shown in Figure 1. Similarly, for the compound **RHB3** which shows low fluorescence intensity in EtOAc, DMSO, and acetone, respectively as shown in Figure 3.

**RHB1** compound was synthesized by the reaction of the rhodamine B and amine (2-amino-5-{4-bromophenyl}-1, 3, 4-thiadiazole) which contains phenyl ring with para directing electron donating group *i.e.*, bromo (–Br) as a substituent. Besides, the **RHB2** and **RHB3** compounds

**Table 1.** Photophysical parameters of the **RHB1**, **RHB2**, and **RHB3** in different solvents.

Compound	Solvent	$\lambda_{\text{ex}}$ (nm)	$\lambda_{\text{em}}$ (nm)	Stokes shift ( $\text{cm}^{-1}$ )	$\epsilon$ ( $\text{M}^{-1} \text{ cm}^{-1}$ )	$\Phi$
<b>RHB1</b>	DCM	560	577	526.12	360	0.39
	EtOAc	—	—	—	—	—
	ACN	—	—	—	—	—
	DMF	—	—	—	—	—
	DMSO	565	585	605.09	80	0.15
	MeOH	550	572	699.30	230	0.12
	Acetone	—	—	—	—	—
<b>RHB2</b>	DCM	560	578	556.10	40	0.5
	EtOAc	560	575	465.83	70	0.072
	ACN	558	578	620.10	210	0.19
	DMF	568	592	713.74	1000	0.08
	DMSO	567	578	335.64	100	0.38
	MeOH	552	576	754.83	890	0.46
	Acetone	560	579	585.98	40	0.72
<b>RHB3</b>	DCM	560	581	645.43	630	0.78
	EtOAc	—	—	—	—	—
	ACN	562	581	581.89	30	0.93
	DMF	—	—	—	—	—
	DMSO	—	—	—	—	—
	MeOH	554	574	628.93	290	0.30
	Acetone	—	—	—	—	—

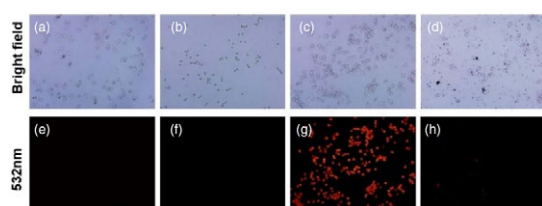


**Figure 4.** Fluorescence imaging studies of live MDA-MB-231 cells. Bright field images of control (a), **RHB1** (b), **RHB2** (c), **RHB3** (d), and fluorescence images of control (e), **RHB1** (f), **RHB2** (g), **RHB3** (h) treated cells are shown. Cells without exposure of samples were considered as control.

were prepared by the reaction of the rhodamine B hydrazide with 4–5 diazafluoren-9-one and 4-amino benzaldehyde, respectively. **RHB1** and **RHB3** both compounds contain an electron donating group attached to phenyl ring such as,  $-\text{Br}$  and  $-\text{NH}_2$ , respectively. **RHB2** shows higher fluorescence response than those of **RHB1** and **RHB3**. It is well-known that rhodamine derivatives can suffer between spirocyclic (non-fluorescent) and open ring (fluorescent) forms.<sup>11,12,15</sup> The reason for the variation in fluorescence properties of **RHB1**, **RHB2**, and **RHB3** lies in the spiro-lactam ring opening mechanism. It might be because of the presence of an electron donating group in the **RHB1** and **RHB3** which opposed the ring opening mechanism. While, in case of **RHB2**, strong fluorescence attributes to a more conjugated fused ring of 4–5 diazafluoren-9-one. In addition to the fluorescence response, the synthesized derivatives further examined for fluorescent cell imaging study in order to categorize the fluorescent response of the respective compounds. Pleasingly, only **RHB2** shows excellent fluorescence image output when it was treated with MDA-MB-231. While other compounds **RHB1** and **RHB3** failed to produce good fluorescent image, it is because of the structural variations and may fails to open spiro-lactam ring in rhodamine core. Additionally, the fluorescence quantum yield of **RHB1**, **RHB2**, and **RHB3** in

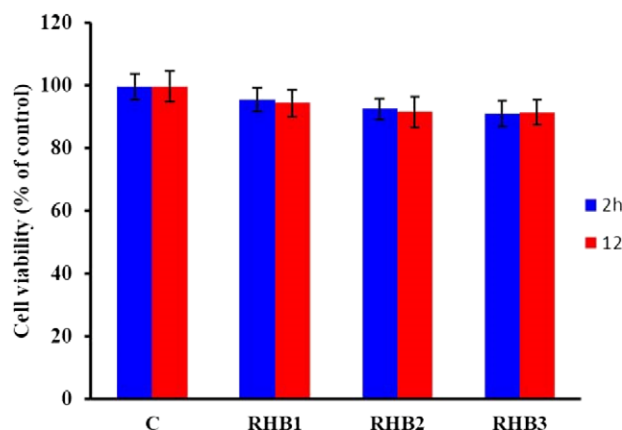


**Figure 5.** Cytotoxicity assessment (MTT assay). Cancer cells (MDA-MB-231 cells) were untreated (Control) and treated with **RHB1**, **RHB2**, and **RHB3** at  $10 \mu\text{M}$  in DMSO for 2 and 12 h.

the different solvents are summarized in Table 1. Remarkable trends for **RHB1**, **RHB2**, and **RHB3** were observed. The quantum yield of **RHB1** reached a maximum of 0.39 in DCM and decreased from 0.15 to 0.12 in DMSO and methanol, respectively. The quantum yield of **RHB2** reached a maximum of 0.5 in dichloromethane but decreased to 0.08, 0.38 in DMF and DMSO, respectively. Similarly, for **RHB3**, the quantum yield was 0.78 in DCM and 0.93 in ACN decreased to 0.32 in methanol. This spectacle can be explained by positive solvatokinetic effect, when the energy level of the excited state reduces in the polar solvent and may cause the reduction in the energy gap and increasing non-radiative transitions, simultaneously. Therefore, we conclude that positive solvatokinetic effect might be the plausible reason for the decrease in fluorescence quantum yield with increase in the polarity of the solvent.<sup>34–36</sup>

**Cell Imaging.** The cancer cells were treated with **RHB1**, **RHB2**, and **RHB3** samples and fluorescence study of each treated sample was performed for MDA-MB-231 cancer cells. Whereas, fluorescence and bright field images of sample was correlated with control (C). The fluorescence investigations were recorded at a wavelength of 532 nm. Experimental results are shown in Figure 4 which indicate that **RHB2** exhibited superior fluorescence in comparison to other samples *i.e.*, **RHB1** and **RHB3**.

**Cytotoxicity.** The cytotoxic effects of **RHB1**, **RHB2**, and **RHB3** were evaluated on cancer cells by using MTT assay. The **RHB1**, **RHB2**, and **RHB3** samples were found non-toxic, as they showed no significant toxic effect on cancer cells. Results of the MTT assay are shown in Figure 5. The results obtained in the cytotoxicity study revealed that synthesized rhodamine derivatives could be explored as fluorescent biomarker to trigger the MDA-MB-21 cell due to its non-toxic nature towards a cell line.

## Conclusion

In summary, we synthesized fluorescent dyes based on rhodamine, which displays excellent spectroscopic properties for **RHB2** as compared to those of **RHB1** and **RHB3**. The fluorescence variations of the dyes are well correlated with the polarity of the solvent, which can be used as a resourceful chemo-sensing platform for designing new ratiometric fluorescent chemosensor. The variation in spectroscopic characteristics posed by synthesized compounds was discussed in detail about the polarity of solvent, functional group attached to rhodamine core and five membered spiro-lactam ring opening mechanism. Considering their good photophysical properties, we used these dyes (**RHB1**, **RHB2**, and **RHB3**) for cell imaging and cytotoxicity experiment against the MDA-MB-231 cancer cell. Furthermore, the fluorescent cell imaging experiment reveals that **RHB2** shows excellent fluorescent triggering responses as compared to **RHB1** and **RHB3**. Thus, noteworthy properties of synthesized derivatives can be explored as attractive

applications as ecologically sensitive fluorescent probes and labels in biology.

**Supporting Information.** Additional supporting information is available in the online version of this article.

### References

1. X. Zhang, Y. Xiao, X. Qian, *Angew. Chem. Int. Ed.* **2008**, *47*, 8025.
2. (a) P. G. Mahajan, N. C. Dige, B. D. Vanjare, Y. Han, S. J. Kim, S. K. Hong, K. H. Lee, *Sensors Actuators B* **2018**, *267*, 119. (b) P. G. Mahajan, N. C. Dige, B. D. Vanjare, S. H. Eo, S. J. Kim, K. H. Lee, *Spectrochimica Acta A: Mol. Biomol. Spect.* **2019**, *216*, 105.
3. P. Krawczyk, B. Jedrzejewska, M. Pietrzak, T. Janek, *J. Photochem. Photobiol. B* **2016**, *166*, 74.
4. K. T. Wong, R. T. Chen, F. C. Fang, C. C. Wu, Y. T. Lin, *Org. Lett.* **2005**, *7*, 1979.
5. W. Z. Yuan, Y. Gong, S. Chen, X. Y. Shen, J. W. Y. Lam, P. Lu, Y. Lu, Z. Wang, R. Hu, N. Xie, H. S. Kwok, Y. Zhang, J. Z. Sun, B. Z. Tang, *Chem. Mater.* **2012**, *24*, 1518.
6. E. Pusztai, I. S. Touloukhonova, N. Temple, H. Albright, U. I. Zakai, S. Guo, I. A. Guzei, R. Hu, R. West, *Organometallics* **2013**, *32*, 2529.
7. P. S. Beaumont, D. G. Johnson, B. J. Parsons, *J. Chem. Soc. Faraday Trans.* **1993**, *89*, 4185.
8. J. Fan, M. Hu, P. Zhan, X. Peng, *Chem. Soc. Rev.* **2012**, *42*, 29.
9. P. Pal, H. Zeng, G. Durocher, D. Girand, T. Li, A. K. Gupta, R. Giasson, L. Blanchard, L. Gaboury, A. Balassy, C. Turmel, A. Laperriere, L. Villeneuve, *Photochem. Photobiol.* **1996**, *63*, 161.
10. M. Cizkova, L. Cattiaux, J. M. Mallet, E. Labbe, O. Buriez, *Electrochim. Acta* **2018**, *260*, 589.
11. Z. Yang, M. She, J. Zhang, X. Chen, Y. Huang, H. Zhu, P. Liu, J. Li, Z. Shi, *Sensors Actuators B* **2013**, *176*, 482.
12. Z. Xu, L. Zhang, R. Guo, T. Xiang, C. Wu, Z. Zheng, F. Yang, *Sensors Actuators B* **2011**, *156*, 546.
13. Y. A. Son, J. Park, *Textile Color Finish* **2012**, *24*, 158.
14. J. Zhang, L. Zhang, Y. Zhou, T. Ma, J. Niu, *Microchim. Acta* **2014**, *180*, 211.
15. J. Chen, W. Liu, B. Zhou, G. Niu, H. Zhang, J. Wu, Y. Wang, W. Ju, P. Wang, *J. Org. Chem.* **2013**, *78*, 6121.
16. H. J. Chen, X. B. Zhou, A. L. Wang, B. Y. Zheng, C. K. Yeh, J. D. Huang, *Eur. J. Med. Chem.* **2018**, *145*, 86.
17. X. Chen, T. Pradhan, F. Wang, J. S. Kim, J. Yoon, *Chem. Rev.* **2012**, *112*, 1910.
18. V. P. Boyarskiy, V. N. Belov, R. Medda, B. Hein, M. Bossi, S. W. Hell, *Chem. Eur. J.* **2008**, *14*, 1784.
19. J. Liu, Z. Diwu, W. Y. Leung, Y. Lu, B. Patch, R. P. Haugland, *Tetrahedron Lett.* **2003**, *44*, 4355.
20. S. Pal, M. Mukherjee, B. Sen, S. Lohar, P. Chattopadhyay, *RSC Adv.* **2014**, *4*, 21608.
21. P. G. Mahajan, N. C. Dige, B. D. Vanjare, H. Raza, M. Hassan, S. Y. Seo, S. K. Hong, K. H. Lee, *J. Fluoresc.* **2018**, *28*, 1305.
22. A. M. Brouwer, *Pure Appl. Chem.* **2011**, *83*, 2213.
23. A. R. Phull, M. Majid, I. U. Haq, M. R. Khan, S. J. Kim, *Int. J. Biol. Macromol.* **2017**, *97*, 468.
24. A. R. Phull, S. H. Eo, S. J. Kim, *Cell. Mol. Biol.* **2017**, *63*, 12.
25. Y. Xiang, L. Mei, N. Li, A. Tong, *Anal. Chim. Acta* **2007**, *581*, 132.
26. B. D. Vanjare, P. G. Mahajan, M. Hassan, H. Raza, S. Y. Seo, S. K. Hong, K. H. Lee, *J. Fluoresc.* **2018**, *28*, 1295.
27. H. Kim, S. Wang, Y. A. Son, *Textile Color Finish* **2012**, *24*, 153.
28. E. Bozkurt, H. I. Gul, E. Mete, *J. Photochem. Photobiol. A: Chem.* **2018**, *352*, 35.
29. J. Papadopoulos, K. Merckens, T. J. J. Meller, *Chem. Eur. J.* **2018**, *24*, 974.
30. A. B. Ormond, H. S. Freeman, *Dyes Pigments* **2013**, *96*, 440.
31. S. Meng, Z. Xu, G. Hong, L. Zhao, Z. Zhao, J. Guo, H. Ji, T. Liu, *Eur. J. Med. Chem.* **2015**, *92*, 35.
32. R. Payal, M. K. Saroj, N. Sharma, R. C. Rastogi, *J. Lumin.* **2018**, *198*, 92.
33. S. Ghosh, N. Roy, T. S. Singh, N. Chattopadhyay, *Spectrochim. Acta A: Mol. Biomol. Spectro.* **2018**, *188*, 252.
34. H. Homocianu, A. Airinei, D. O. Dorohoi, *J. Adv. Res. Phys.* **2011**, *2*, 1.
35. B. Varghese, S. N. Al-Busafi, F. O. Suliman, S. M. Z. Al-Kindy, *J. Lumin.* **2015**, *159*, 9.
36. Z. Zhang, P. Xue, P. Gong, G. Zhang, J. Peng, R. Lu, *Mater. Chem. C* **2014**, *2*, 9543.